Journal of The Electrochemical Society, 2022 **169** 092510

Characteristics of Anode Materials for Nickel Electroforming

T. A. Green,[z] C. Enowmbi Tambe, and S. Roy

Department of Chemical and Process Engineering, University of Strathclyde, Glasgow, Scotland G1 1XJ, United Kingdom

This study comprised an investigation of the characteristics of commercial nickel anode materials routinely employed in sulfamate-based electroforming processes. These included examples of sulfur depolarised anodes containing a relatively high sulfur content and those with much lower levels. Electrochemical studies indicate that the sulfur depolarised anodes underwent dissolution in the active region and were capable of sustaining large current densities at low potentials without passivating, and with current efficiencies approaching 100%. In contrast, low-sulfur containing anodes could only sustain low current densities in the active region, and were prone to passivation. These materials could only undergo high rate dissolution in the transpassive region, but this required relatively high anode potentials and was accompanied by various side reactions which lowered the current efficiency. Additional studies were performed to characterise the sulfamate oxidation products which generates a distinct UV absorption band at 245 nm. These species were produced only when low-sulfur content or inert (platinum) anodes were used, and were absent when sulfur depolarised anodes were employed. The principal anode product was azodisulfonate, but trace amounts of other sulfonate species and sulfur-containing anions may also be present.

 [DOI: 10.1149/1945-7111/ac8ee9]

Manuscript submitted June 20, 2022; revised manuscript received August 23, 2022. Published September 9, 2022.

Electroforming is an additive manufacturing technique capable of producing high precision metallic components from the macro to micro-scale. It is usual defined as "the production or reproduction by electrodeposition of articles upon a mandrel or mould that is subsequently separated from the deposit."[1] In this manner, complex shapes with high dimensional tolerances can be obtained. For manufacturing at the macro-scale it has been used to prepare components as diverse as nozzles and thrust chambers for rockets,[2] erosion shields for helicopter blades[3] and X-ray mirrors for ground and spaced-based telescopes.[4] Importantly, these components could not be easily, or economically, fabricated by conventional process such as casting, forging stamping or machining, and electroforming remains the only viable option. More recent applications of electroforming include the fabrication of meso-scale parts such as foils, sieves, reticules, masks, gratings and stampers for CDs, DVDs and Blu-ray disks.[5,6] The scope and importance of electroforming is apparent from a number of recent review articles[7–10] and in 1999 the global market size was estimated to exceed 2 billion U.S. dollars.[10]

Since the early 1980s electroforming has been extended into the domains of micro and nano-manufacturing.[9] This initially started with the development of the LIGA process,[11] and the technique of through-mask plating,[12] both of which can be used to produce high aspect ratio metal micro-parts. Electroforming is now routinely used in microfabrication to various MEMs devices such as cantilevers, micro-mirrors, ink-jet nozzles, micro-motors and micro-optic components.[13] It is also used to produce stamps and moulds to facilitate the fabrication off micro- and nano-structures[13] and has applications in wafer level packaging.[14] Electroforming is therefore one of the few manufacturing technologies which can fully encompass the macro- to nano-fabrication domains.

While gold can also be electroformed, nickel and copper are the most widely used metals in industry.[8,9] In the latter case, it is mainly restricted to the production of copper foils for PCB manufacture, whereas the applications of nickel electroforming are much more diverse.[10] Particularly since the development of the sulfamate plating process, which allows high deposition rates and very low deposit stress, nickel electroforming has dominated most industrial applications.[6,15] The nickel sulfamate process also has excellent throwing power which is essential for maintaining a uniform thickness across the electroformed part. It is one of the best studied and understood electrodeposition processes and a number of reviews are available[15–18] which describes its optimisation and control.

A key requirement for electroforming is that the deposit has low stress, so that when the component is released from the mandrel it does not deform and undergo dimensional changes.[5,6,9,10] For this reason most studies of nickel sulfamate have concentrated on achieving and maintaining low stress, although considerations related to the mechanical properties (e.g. hardness,[3] ductility,[3,19] strength[3,9,20] and elastic modulus[20]) and surface roughness[4,12] of the deposit are also important in many applications. Control of deposit stress, microstructure and roughness is mainly related to considerations of the bath composition (e.g. additives, buffers) and the operating condition (e.g. current density, pH, temperature, agitation) and the complex interactions between these variables are well understood.[15–18,21–23]

There has, however, been relatively less attention paid to the role of the anode in nickel electroforming, and most published studies date back to the 1960 – 1990s.[24–28] Since then, new anode materials have become available, and the scope of electroforming has broadened considerably. The nickel sulfamate process typically employs various types of soluble nickel anodes, and their characteristics can be very different. Ideally the anode should dissolve uniformly and with 100% Faradaic efficiency, so that the overall nickel content is kept constant, and there are no side reactions which can introduce additional species into the bath or change the pH.[15–17] In reality, many types of Ni anodes are not 100% efficient and various side reactions have been demonstrated to occur.[24–28] Preferably, the anode should dissolve in the active state, but under certain conditions it can passivate, and transpassive dissolution is also possible.[15,29,30] Importantly, products due to the anodic decomposition of sulfamate ions are known to influence the cathodic deposition process.[6,14,25–27] Although this can be beneficial in some cases, for example by reducing stress, these additives are essentially being introduced into the plating bath in an uncontrolled manner, and their chemical nature is largely unknown.

The first aim of this study is to characterise a wide range of commercially available anode materials. Initially this includes establishing their basic dissolution characteristics via potentiostatic and galvanostatic measurements, identifying the regions where active, passive and transpassive dissolution occurs, and determining anodic current efficiencies. The second aim is to assess the formation of sulfamate decomposition products that occur when various types of anode are employed. As noted previously, it is important to identify the conditions under which these species are generated, as they can have a significant effect on the deposition process and deposit characteristics.

[z]E-mail: todd.green@strath.ac.uk

Experimental

Anode Materials.—Essentially two types of nickel anodes were employed in these experiments. The first of these were "electrolytic" (sulfur-depolarised) materials which are pure Ni (99.9–99.95 wt%) but contain sulfur (0.025 wt%) as an impurity. These are prepared by electrodepositing nickel on to a mandrel sheet. These anodes are capable of dissolving at 100% current efficiency (CE) even in the absence of chloride in the solution. The materials used here D-Crowns (Nikkelverk) and S-Rounds (Vale). However, the latter product is not currently being manufactured by Vale and has been replaced by S-Pellets. These pellets have a similar sulfur content, but are manufactured by a modified Mond process where carbonyl sulphide is added to incorporate sulfur. S-Pellets are not homogenous alloys, having a modulated sulfur content and microstructure, but possess similar dissolution characteristics to S-Rounds.[31]

The second type of anode used were high-purity nickel materials formed by a standard carbonyl (Mond) process. These materials have a low sulfur content (<0.0002 wt%) and high Ni purity (99.98 wt%) and typically require the sulfamate solution to contain chloride ions to avoid anode passivation and maintain a high current efficiency. The materials used in this study where P-Pellets (Vale) and Nickel Plating Chips (Vale). These have a similar chemical composition but different sizes and shapes. Nickel anodes produced by the carbonyl process typically have a laminar structure, with each layer exhibiting variations in composition and microstructure. The composition and form of all anode materials used is summarised in Table I.

In order to facilitate electrochemical measurements, the D-Crowns, S-Rounds and Plating Chips were ground into disk shaped specimens that could be fitted into a PEEK sample holder (Origalys) and used as a rotating disk electrode (RDE). This allowed the anode materials to be characterised under stationary or hydrodynamic conditions and assess the importance of mass transport limitations on dissolution characteristics. The area exposed to the solution was 1.35 cm^2. In the case of the S-Pellets and P-Pellets, these could not be easily machined into RDE-compatible disks, and were consequently used in their original spherical form. These anode materials could therefore only be characterised under stationary conditions. The areas of the pellets were approximately 4 cm^2, and precise areas were based on dimensional measurements with a Vernier calliper. Electrical contact was made to the pellets by tapping a small hole and then inserting a threaded titanium rod. This allowed for a reliable and low resistance (<0.1 Ω) contact. For experiments with an inert anode, a coil of Pt wire was used with a working area of 4.8 cm^2.

Prior to the experiments being performed, the nickel anodes were polished with 1200, 2400 and 4000 grade silicon carbide paper, rinsed in DI water, and then dried under a stream of nitrogen. This facilitated the formation of reproducible and film-free surfaces. For the disk samples, this was performed on a polishing machine (Struers DAP-7), but the pellets were polished manually.

Electroforming Solution.—In all experiments a nickel sulfamate solution was used that corresponded closely to that employed in industrial situations. The bath was formulated from AR grade reagents and had a composition of: 1.785 M $Ni(SO_3NH_2).4H_2O$ + 0.020 M $NiCl_2.6H_2O$ + 0.65 M H_3BO_3. It did not contain any wetting agent or any proprietary additives. The initial pH of the solution was 3.3 and all experiments were performed at 45 °C. Additionally, some experiments were performed in the absence of $NiCl_2$ to ascertain the importance of chloride ions in promoting dissolution and minimising anode passivation. Other factors such as the pH and the boric acid concentration can also influence anode passivity in sulfamate and Watts baths but these factors were not explored.[30,32]

Electrochemical Experiments.—Electrochemical experiments involving the various anode materials were performed in a single compartment jacketed cell with a volume of 70 ml. A thermostatic bath was used to pump water through the jacket so the cell could be maintained at a temperature of 45 °C. Polarisation were performed using a potentiostat (PGSTAT30, Metrohm Autolab) in a conventional three-electrode configuration. The working electrode consisted of the various anode materials, the counter electrode was a Pt wire counter electrode (0.35 cm^2) and a SCE was employed as the reference electrode.

As the measured current densities were often high (>10 mA cm^{-2}) *IR* compensation by positive feedback was required to minimise distortion of the polarisation data. The value of the uncompensated resistance, *R*, was obtained using a combined potentiostat and impedance analyser (Palmsens 4) and 90% of this value was applied during each scan. This level of compensation was chosen to provide relatively high levels of *IR* correction without risking the potentiostat instability and oscillations that invariably occur close to 100% compensation. The potential was scanned between the open circuit potential and +1.6 V versus the SCE and the scan rate was 5 mV s^{-1} to maintain steady-state conditions. Some additional experiments were performed galvanostatically to analyse the active, passive and transpassive characteristics of the anodes. Typically in these experiments, fixed current densities (1–25 mA cm^{-2}) were applied and the anode potential monitored as a function of time.

A limited number of experiments were performed under hydrodynamic conditions to determine if solution agitation had any influence on anodic dissolution. To facilitate this, the PEEK sample holder was attached to an EDI101 electrode rotator and CTV101 controller (Radiometer Analytical), and rotated at a speed of ω = 0–900 rpm. When required, current efficiencies were determined by weighing the nickel anode (±0.1 mg precision) before and after the dissolution experiments.

Sulfamate Decomposition Experiments.—These experiments employed the same 70 ml single compartment cell used in the electrochemical experiments. They were performed galvanostatically,

Table I. Summary of chemical compositions (in wt%) and forms of nickel anode materials. Information taken from the technical datasheet for each material.

	S-Rounds	D-Crowns	S-Pellets	P-Pellets	Plating chips
Ni	>99.90	>99.95%	>99.97	>99.98	>99.98
S	0.019−0.025	0.018−0.030	0.022−0.030	<0.0002	<0.0002
Co	<0.065	<0.0002	<0.00002	<0.00002	<0.00002
Cu	<0.0008	<0.0001	<0.0001	<0.0001	<0.0001
C	<0.0035	<0.002	<0.005	<0.011	<0.007
Fe	<0.0003	<0.001	<0.004	<0.004	<0.004
Pb	<0.0003	<0.0002	$<10^{-6}$	$<10^{-5}$	$<3 \times 10^{-6}$
Zn	<0.0002	<0.0002	<0.00002	<0.00002	<0.00002
Form	Button	Button	Spherical	Spherical	Plate
Manufacturing Process	Electrolytic	Electrolytic	Modified Carbonyl	Carbonyl	Carbonyl

with current densities of 5−25 mA cm^{-2} applied between the various anode materials and a 304-grade stainless steel cathode (1.35 cm^2) rotating at $\omega = 450$ rpm. The recommended anode to cathode area in electroforming is normally 2:1 so this would simulate conditions where the cathodic current density was typically 10–50 mA cm^{-2}. The stainless steel cathode allowed the deposition of nickel in a controlled way and under realistic electroforming conditions but the deposit was not characterised any further. However, gravimetric analysis indicated that Ni was depositing at around 100% current efficiency and visually it had the appearance of a smooth and coherent deposit.

UV-Visible Spectroscopy.—Spectra of the nickel sulfamate solutions were recorded using a Varian Cary 5000 UV–vis-NIR spectrometer over the wavelength range 200–800 nm. The data interval and integration time where 1 nm and 0.1 s, respectively, resulting in a scan rate of 600 nm min^{-1}. Samples were taken from the electrochemical cell as required, and analysed without further dilution in a 1 mm path length quartz cuvette. Unless stated otherwise, all spectra were referenced against a cuvette containing pure water. The samples were maintained at temperature before each measurement to minimise errors due to the precipitation of boric acid.

For the thermal decomposition studies, sealed nickel sulfamate samples which had been electrolysed previously were heated on a hotplate at 67 °C with stirring. Aliquots were then taken at regular time intervals and the UV–vis spectrum was monitored in the range 200–800 nm to detect any changes.

Results and Discussion

Electrochemical Studies.—Initial polarisation scans to evaluate the anodic characteristics in a nickel sulfamate solution containing 1.785 M $Ni(SO_3NH_2).4H_2O$, 0.020 M $NiCl_2.6H_2O$ and 0.65 M H_3BO_3 are shown in Fig. 1. These scans show rather different characteristics of the two different types of anode materials, although both exhibit distinct active, passive and transpassive regions. The critical current density for passivation is typically two orders of magnitude lower for the low-sulfur anodes, and sulfur-depolarised anodes can therefore support much large current densities than the low-sulfur anodes in the active region before undergoing passivation. These findings are in good agreement with previous studies[19,32,33] of sulfur-depolarised and low-sulfur anodes in sulfamate baths.

The influence of the nickel anode composition and microstructure on dissolution characteristics has been previously noted.[34–37] In an early study by Di Bari[34] the anodic characteristics of nickel in acidic sulfate media were shown to depend significantly on microstructure (modified by annealing and work hardening) but was dominated by presence of certain impurities, particularly sulfur. For this reason, anode suppliers have found varying the sulfur content as the most practical method of modifying dissolution characteristics. Additional complications also arise due to the non-homogenous (laminar) characteristics of most nickel formed by carbonyl process (e.g. S and P-Pellets). Studies[35,36] have shown that these layers have compositional and microstructure differences (especially grain size and shape) and these have a significant influence on dissolution characteristics. In practice, the layers often dissolve preferentially producing thin, hemispherical anode residues.[37] The observed differences in polarisation behaviour in Fig. 1 are therefore not unexpected given the compositional and microstructural variations arising from the different anode manufacturing routes.

Figure 2 shows the polarisation data for the sulfur-depolarised anodes in the presence and absence of chloride. All anode materials can support active nickel dissolution between −0.1 V to +0.2 V versus SCE, but the current density subsequently declines and at potential of +0.7–+1.0 V they are fully passive. At potentials above +1.3 V the passive film breaks down and transpassive dissolution commences. Note that the dissolution behaviours of the D-Crowns and S-Rounds are broadly similar and any variations probably reflect compositional and microstructural differences. The S-Pellet also exhibits some differences from the S-Rounds—again reflecting a different manufacturing process and the resulting compositional and microstructural variations.

Nevertheless, all anodes types are capable of supporting very large dissolution currents (>100 mA cm^{-2}) in the active region at relatively low potentials. The presence of chloride improves the characteristics of all anodes (Fig. 2) but it is clear that sulfur-depolarised materials do not require chloride to facilitate dissolution. These results are in good agreement earlier studies[19,32,33] which reported broadly similar polarisation characteristics with sulfur-depolarised anodes. Various electroforming reviews[15–18] also state that sulfur-depolarised anode materials can be operated in chloride-free solutions and the datasheets for these products also support this view.

Figure 3 summarises the polarisation data for the low-sulfur content anode materials in the presence and absence of chloride. These materials also exhibit an active dissolution region between −0.1 V to +0.3 V but in contrast to the sulfur-depolarised ones can only sustain relatively low current densities (< 3 mA cm^{-2}). At potentials more anodic than +0.3 V, the anodes are fully passive due to the formation of various nickel oxides, but beyond +1.3 V these breakdown and transpassive dissolution commences. In accordance with previous studies[32] the presence of chloride does not substantially change the polarisation characteristics of the anodes, but there is a slight improvement in dissolution characteristics. In nickel sulfate baths, chloride is effective in inducing passive film breakdown at lower potentials, but this is not the case in sulfamate electrolytes.[32] Moreover, higher levels of chloride are considered undesirable in sulfamate baths, as they tend to increase tensile stress[10,17,24] and may cause non-uniform dissolution (e.g. pitting) of the anode.

These initial results indicate that, if low sulfur content anodes are to be employed at reasonable current densities (i.e. > 5 mA cm^{-2}) they are likely to be undergoing transpassive rather than active dissolution. These findings are in good agreement with earlier electrochemical studies[32,33] that indicate that low-sulfur anode materials typically undergo transpassive dissolution at a relatively high potential in nickel sulfamate solutions. To ensure dissolution in the active region would typically require low current densities. This is indicated in the chronopotentiometry experiment shown in Fig. 4, which displays the time response of the anode potential when various current densities are applied to a P-Pellet. In most cases, the potential shifts from active to transpassive dissolution after a relatively short transition time (<50 s). Only at very low current densities (<0.5 mA cm^{-2}) does dissolution continue in the active region for extended periods.

The use of low-sulfur anodes in sulfamate solutions is feasible, but there are a number of issues to consider. Firstly, the potential will be very much higher than for active (sulfur depolarised) anodes and there will be a very substantial increase in the cell voltage and therefore energy consumption. Previous studies[37,38] have shown that, depending on the current density and other process conditions, sulfur-depolarised anodes can reduce energy consumption by 5–30%. Secondly, a number of other reactions can occur during transpassive dissolution, for example, the oxidation of sulfamate ions[25–28,33] or water.[29] In the latter case, the reversible potential for O_2 evolution at pH = 3.3 is $E_r = 0.80$ V vs SCE so this reaction is thermodynamically feasible in the potential range investigated. Both of these reactions can cause additional complexities in the process, and will result in a lower anodic current efficiency.

A systematic study of current efficiencies was not undertaken but galvanostatic and potentiostatic experiments indicated that in the active region it was close to 100% at all current densities for both sulfur-depolarised and low-sulfur anodes. In contrast, for transpassive dissolution of low-sulfur anodes it was typically of the order of 50–95% and depended on the current density. Some representative current efficiency data for the two types of anodes is summarised in Table II.

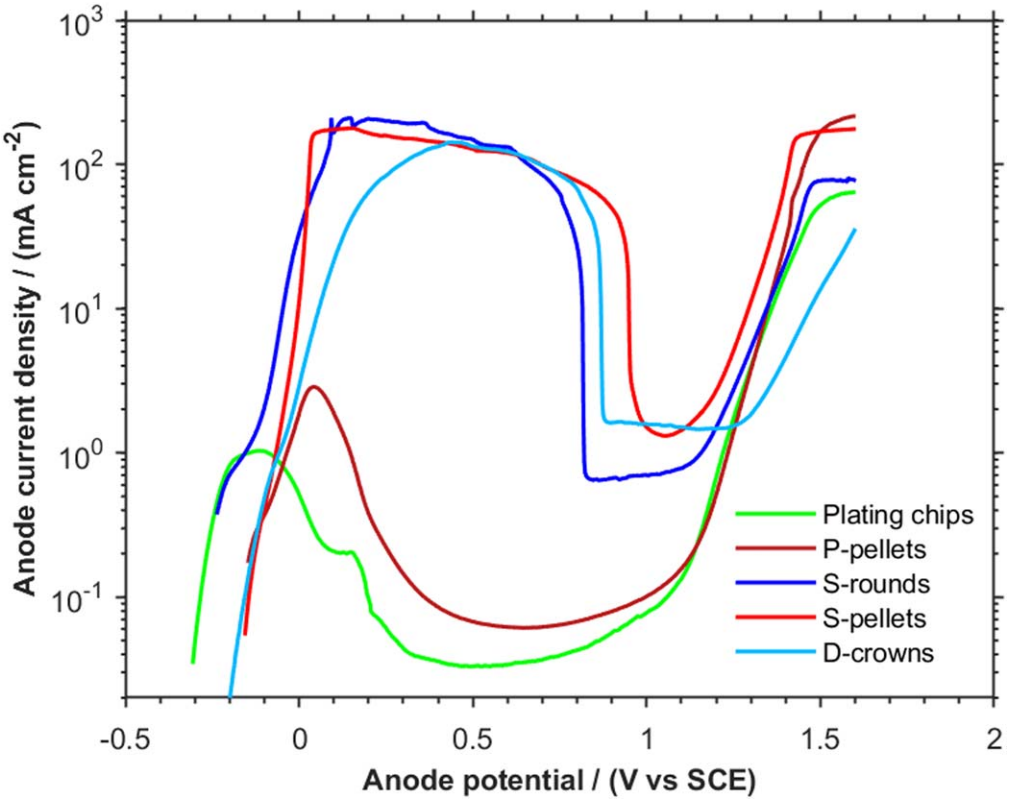

Figure 1. Polarisation plots for the various types of nickel anode materials at a scan rate of 5 mV s^{-1} illustrating active, passive and transpassive regions. The base electrolyte compromised 1.785 M $Ni(SO_3NH_2).4H_2O$, 0.020 M $NiCl_2.6H_2O$ and 0.65 M H_3BO_3.

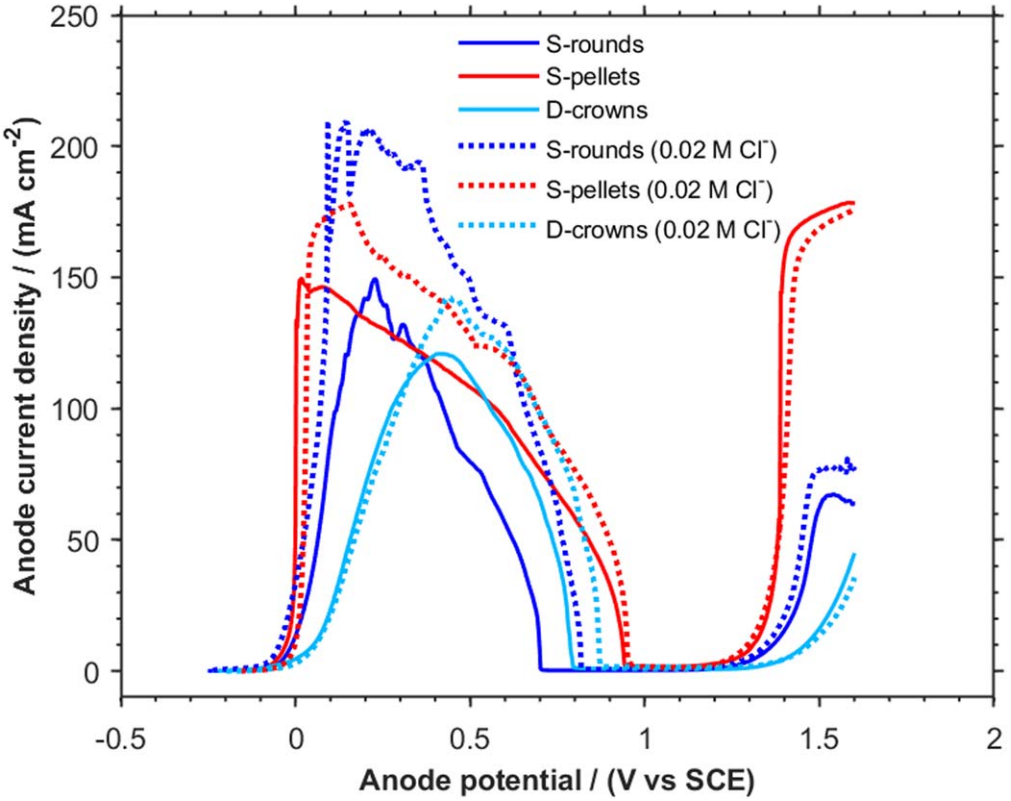

Figure 2. Influence of chloride ions on the polarisation plots for the sulfur-depolarised anode materials at a scan rate of 5 mV s^{-1}. The electrolyte compromised 1.785 M $Ni(SO_3NH_2).4H_2O$, 0.65 M H_3BO_3 with and without 0.02 M $NiCl_2.6H_2O$.

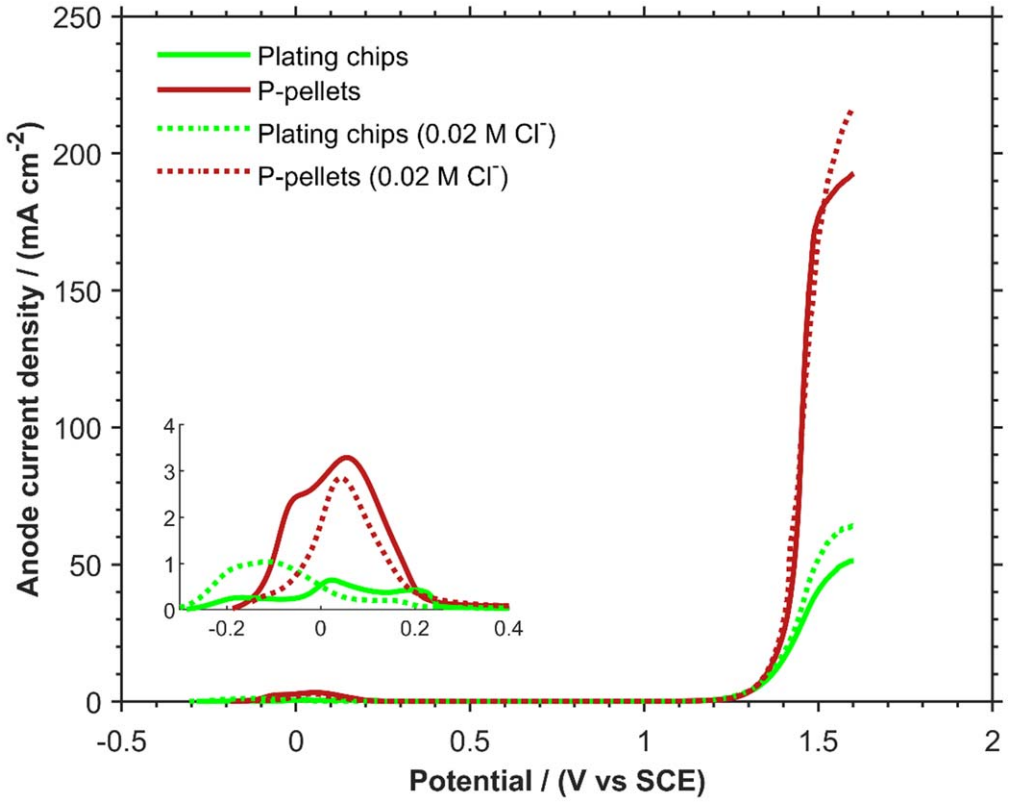

Figure 3. Influence of chloride ions on the polarisation behaviour of low-sulfur anode materials at a scan rate of 5 mV s^{-1}. The electrolyte compromised 1.785 M $Ni(SO_3NH_2).4H_2O$, 0.65 M H_3BO_3 with and without 0.020 M $NiCl_2.6H_2O$. The zoomed insert shows the active/passive region in more detail.

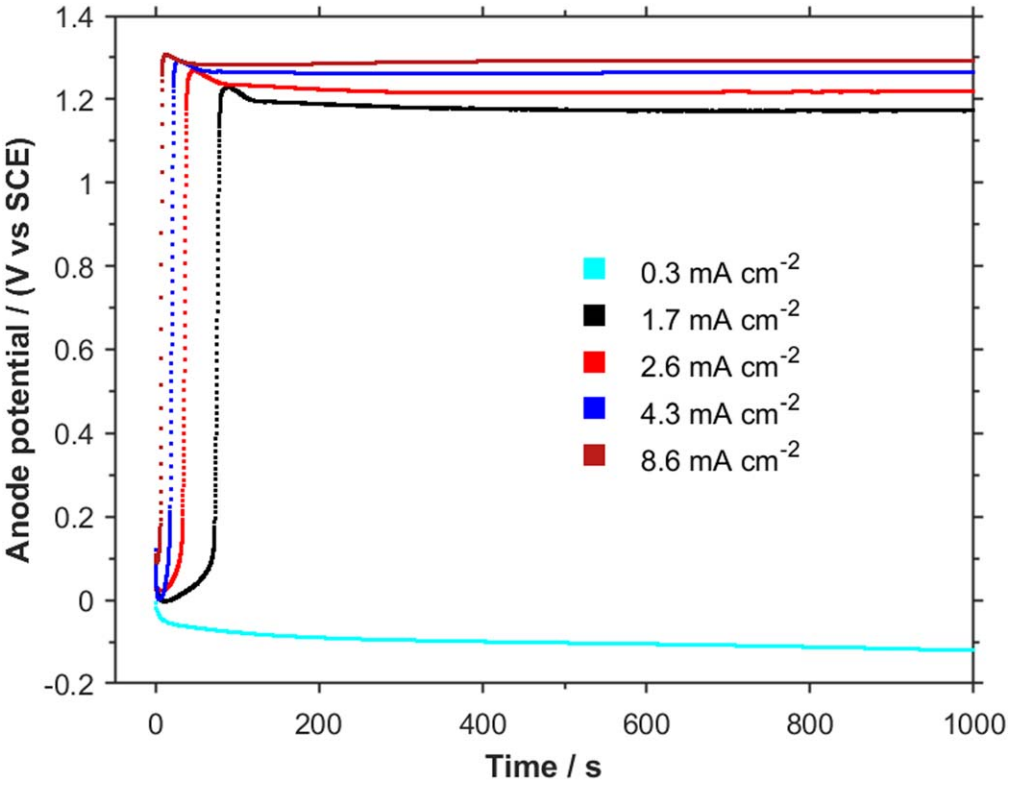

Figure 4. Time dependence of the anode potential when various current densities are applied to a P-pellet.

A final investigation examined the effect of solution agitation on the anodic polarisation characteristics. As noted earlier, this was only possible for the anode materials that could be formed into a RDE sample. The effect of electrode rotation on the low-sulfur anodes (Fig. 5) resulted in higher dissolution current densities in both the active and transpassive regions clearly showing the

Table II. Summary of anodic current efficiencies (%CE) and potentials (*E*) for dissolution of two types of nickel anodes and the platinum anode at various current densities. Total charge passed was 500 C. For the S-pellet, dissolution occurred in the active region; for the P-Pellet in the transpassive region.

	S-Pellet		P-Pellet		Pt	
j mA cm^{-2}	%CE	*E*/V	%CE	*E*/V	%CE	*E*/V
5	98.0	−0.04	82.3	1.26	—	1.99
10	99.6	−0.05	64.1	1.44	—	2.05
25	97.3	−0.01	49.3	1.42	—	2.11

importance of mass transport effects. Solution agitation can therefore extend the current density range which these anodes could be used in the active region and reduce the risk of passivation. For the sulfur-depolarised anodes, there was also a significant increase in the active dissolution current density with rotation rate. The potential range over which active dissolution could occur was extended, while the range for passivity was substantially reduced (Fig. 6). However, even in unstirred solutions these anodes can sustain high current densities (>100 mA cm^{-2}). Such high values are unlikely to be realised under normal electroforming conditions so the benefit of agitation in this case is relatively minor.

The effect of mass transport on dissolution in the active-passive region has been studied previously for iron and nickel.[29] A classic example is the dissolution of iron in sulfuric acid where a limiting peak passivation current density is often observed due to the precipitation of a pre-passive $FeSO_4$ salt film.[39] For nickel dissolution under similarly acidic conditions a limiting current is also obtained, but it arises from the formation of a pre-passive NiO or $Ni(OH)_2$ layer on the surface rather than a salt film.[40–42] According to Sato,[41] in the active dissolution region the overall reaction is: $Ni + OH^- \rightarrow NiOH^+ + 2e-$, but as the surface concentration of $NiOH^+$ reaches its saturation value, NiO will precipitate according to: $NiOH^+ \rightarrow NiO + H^+$. The surface concentration of $NiOH^+$ will be reduced at higher rotation rates allowing a higher passivation current, and this is in qualitative agreement with the results shown in Figs. 5 and 6.

Anode Decomposition Products.—Following the electrochemical studies, an analysis was undertaken to detect decomposition products formed by the oxidation of sulfamate ions at the anode. These decomposition products typically generate a broad UV absorption band at 245 nm.[14,25,27,33] Nickel sulfamate solutions exhibit distinct absorption bands at 215 nm, 400 nm, 640 nm and 730 nm[43] which are characteristic of uncomplexed Ni^{2+} ion in aqueous solution, and these do not significantly overlap with the 245 nm peak. The assignment of the peak is contentious, and has been attributed to various sulfonate species.[25,27,28,33] These studies have shown that this species is typically generated when inert (platinum) or low-sulfur containing ("un-activated") anodes are used, as it requires the anode to reach potentials sufficient to oxidise the sulfamate.

Subsequent experiments involved studying the conditions under which the peak was present or absent—particularly in relation to the type of anode employed. For these experiment, an S-Pellet was chosen to be representative of a sulfur–depolarised anode, and a P-Pellet as an example of a low-sulfur anode material. Additionally, a platinum wire was used to represent an inert (insoluble) anode. These experiments were performed in a nickel sulfamate bath under typical electroforming conditions, as many earlier studies[25,27,28] of sulfamate oxidation had employed nickel-free sulfamate solutions and/or inert (i.e. Pt or C) electrodes. While such studies are useful, it is not clear that they are representative of actual electroforming processes, which have a more complex bath chemistry and invariably employ soluble nickel anodes.

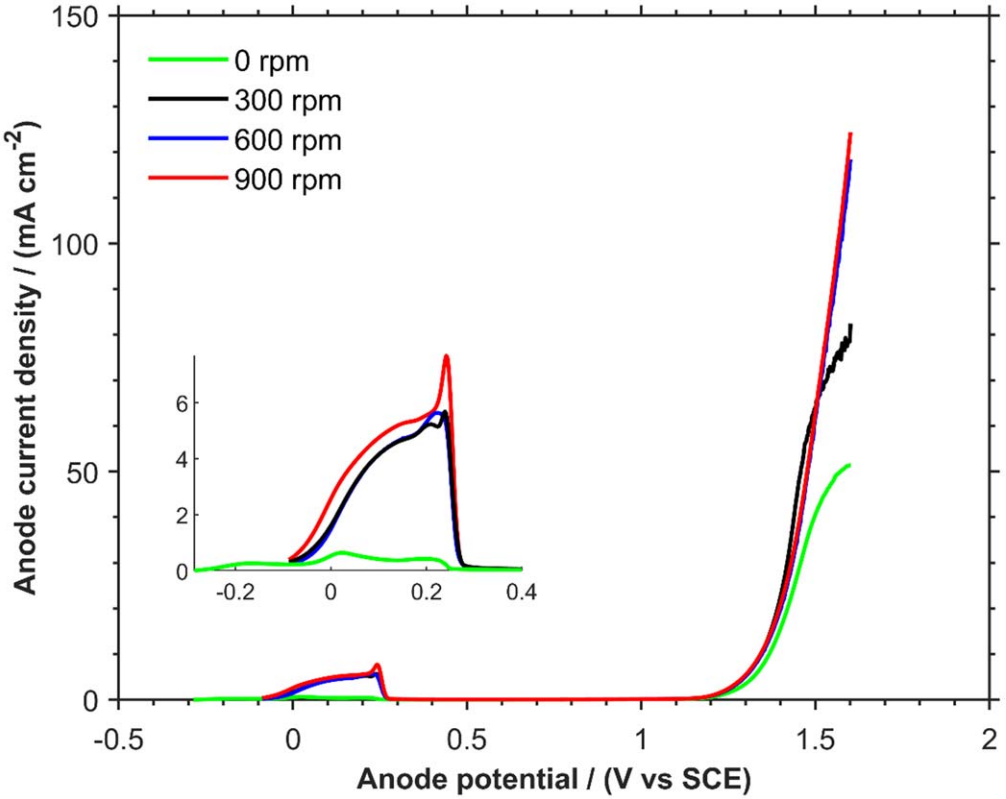

Figure 5. The influence of the electrode rotation rate (ω = 0–900 rpm) on the polarisation curve for a low-sulfur anode material (Plating Chip) in the absence of $NiCl_2$. The zoomed insert shows the active/passive region in more detail.

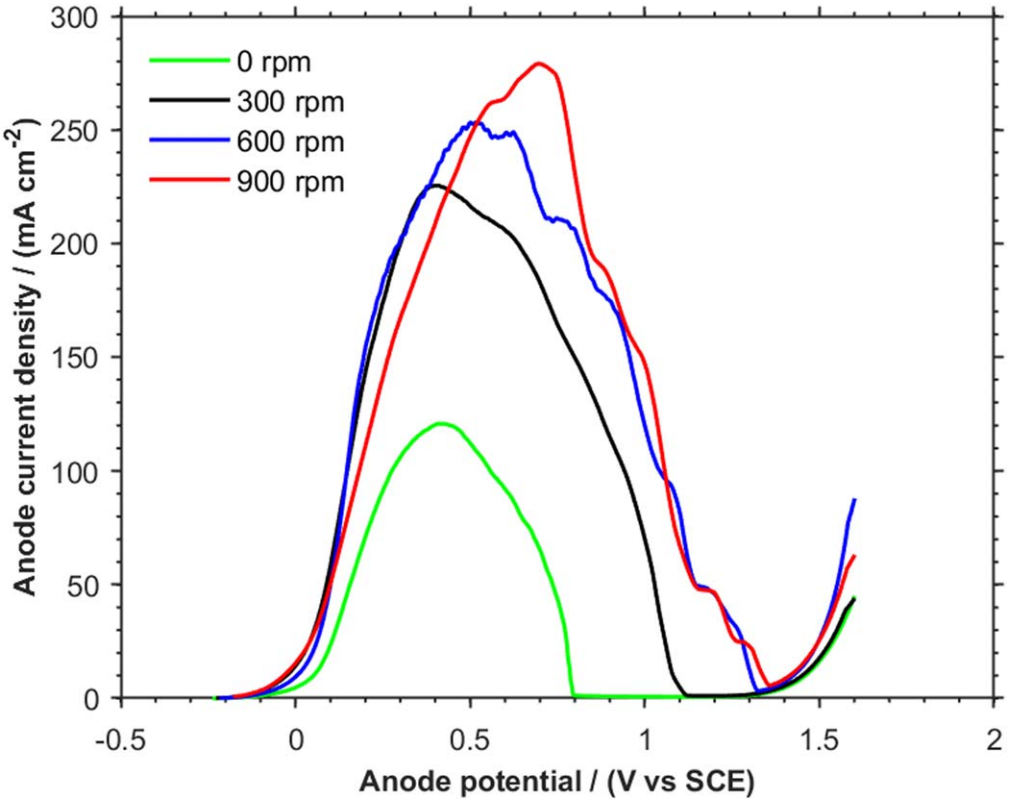

Figure 6. The influence of the electrode rotation rate (ω = 0–900 rpm) on the polarisation curve for a sulfur depolarised anode material (D-Crown) in the absence of $NiCl_2$.

Figure 7 shows the UV–vis spectrum in the small undivided cell for the S-Pellet before electrolysis and after a charge of 500 C was passed. These experiments were performed at current density of 5 and 25 mA cm^{-2} and typically the anode reached a potential of 0.0 V versus the SCE and the anodic current efficiencies measured gravimetrically were 97.5–99.5% (Table II). This figure shows the absence of an absorption peak at 245 nm, suggesting that anodic decomposition of sulfamate does not occur at the anode. Presumably this is because the anode potential does not reach sufficiently high anodic values, and this agrees with the earlier study of Nakano and co-workers.[33]

In contrast, Fig. 8 shows a comparable experiment employing a P-Pellet anode. Current densities of 5–25 mA cm^{-2} were employed but in these cases the anode potential attained a value of 1.25–1.4 V. The current efficiencies were 50–90% (Table II) indicating that other reactions (sulfamate oxidation and possibly O_2 evolution) were also occurring at a significant rate. Notably in this case the 245 nm peak is visible at all current densities, indicating the formation of a sulfamate decomposition product. In this instance the anode potential attains a large enough value to oxidise the sulfamate ion.[33] Figure 9 shows an experiment with the P-Pellet when the current density was fixed at 25 mA cm^{-2} and various amounts of anodic charge were passed. The correlation between the absorbance and the anodic charge, clearly indicates an electrochemical origin for the decomposition product.

An additional experiment was performed using a platinum wire anode (Fig. 10). Conditions were as described previously for the P and S pellets and typically the anode potential attained was 2.0 − 2.5 V. This trial also showed a 245 nm peak consistent with the formation of a sulfamate decomposition product. This is in agreement with prior studies[25,27,28] in nickel-free sulfamate solutions which exhibited a 245 nm peak when carbon or platinum electrodes were employed.

The preliminary conclusions from these initial studies can be summarised as follows. Firstly, if the formation of sulfamate decomposition products are to be avoided under typical electroforming conditions, then sulfur depolarised anodes are mandatory. On the other hand, if low-sulfur or inert anodes are used, sulfamate oxidation will invariably occur. However, this in itself is not necessarily a problem, and the presence of such species are often regarded as being desirable as they can lower deposit stress[6,25–27] and function as brighteners.[14] Additionally, these products can increase the sulfur content in the deposit, reduce the grain size and increase hardness.[33]

In a recent study of a under bump metallization (UBM) process, it was shown that high quality Ni barrier layers could only be obtained from a sulfamate bath when a 245 nm peak was visible, and this required the use of sulfur depolarised anodes.[14] Therefore, in cases where the generation of such products is desirable or necessary, the use of low-sulfur anodes may be preferred. Additionally, sulfur depolarised nickel produce more anode residues than low-sulfur nickel and, due to the formation of surface films, may need regular cleaning and activation to maintain a low anode potential.[37,44] Industrial best practice may therefore favour low-sulfur materials in some instances.

This study was concerned with the characteristics of nickel anodes and their role in facilitating or preventing sulfamate decomposition, and not on the influence of these species on the deposit properties. Nevertheless, some additional experiments were performed to obtain cathodic polarisation curves for nickel deposition at 304-grade stainless steel cathodes in the presence and absence of the decomposition product. Figure 11 shows that there is a systematic change in polarisation behaviour as a function of the amount of the decomposition product present in the electroforming solution. The main effect at low current densities is to reduce the potential required to achieve a particular current density, so the anode product is mainly functioning as a depolariser, but this is reversed at higher current densities (>100 mA cm^{-2}). In the study by Nakano[33] polarisation curves were also measured in the presence and absence of the anode product. The scatter in their data is considerable, but it does suggest that the additive is also acting as a depolariser in the range 0.1–100 mA cm^{-2}. These results are consistent with other Ni

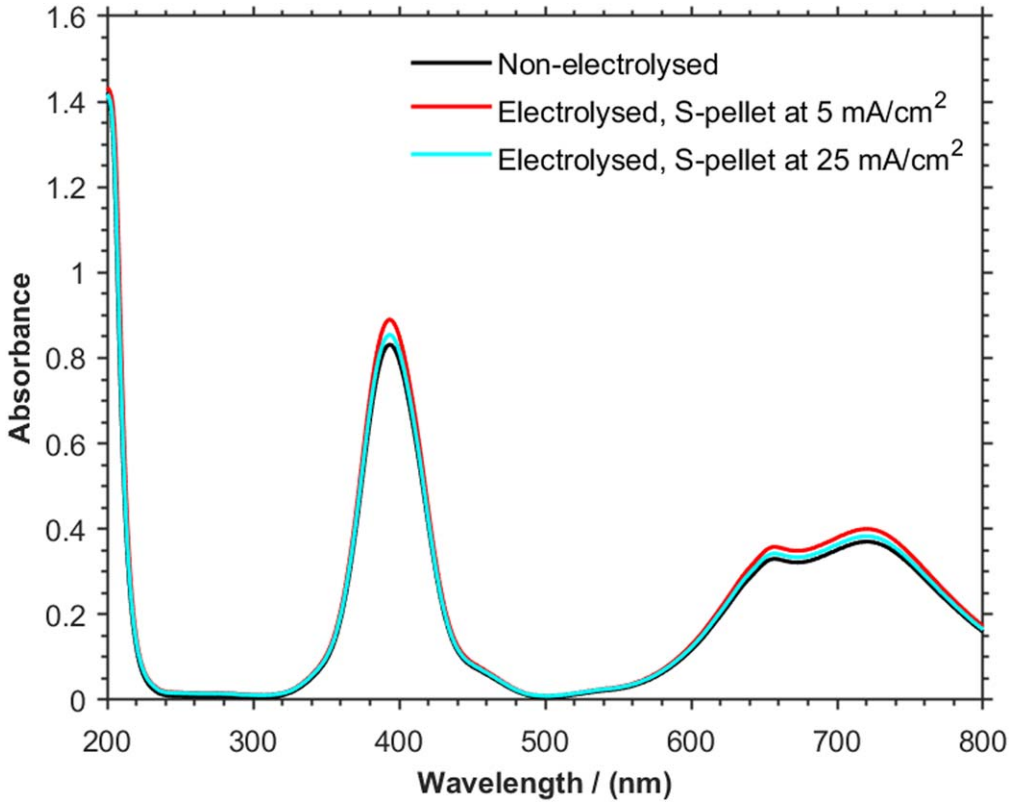

Figure 7. The UV–vis spectra for the S-Pellet before electrolysis and after a charge of 500 C was passed at a current density of 5 and 25 mA cm^{-2}.

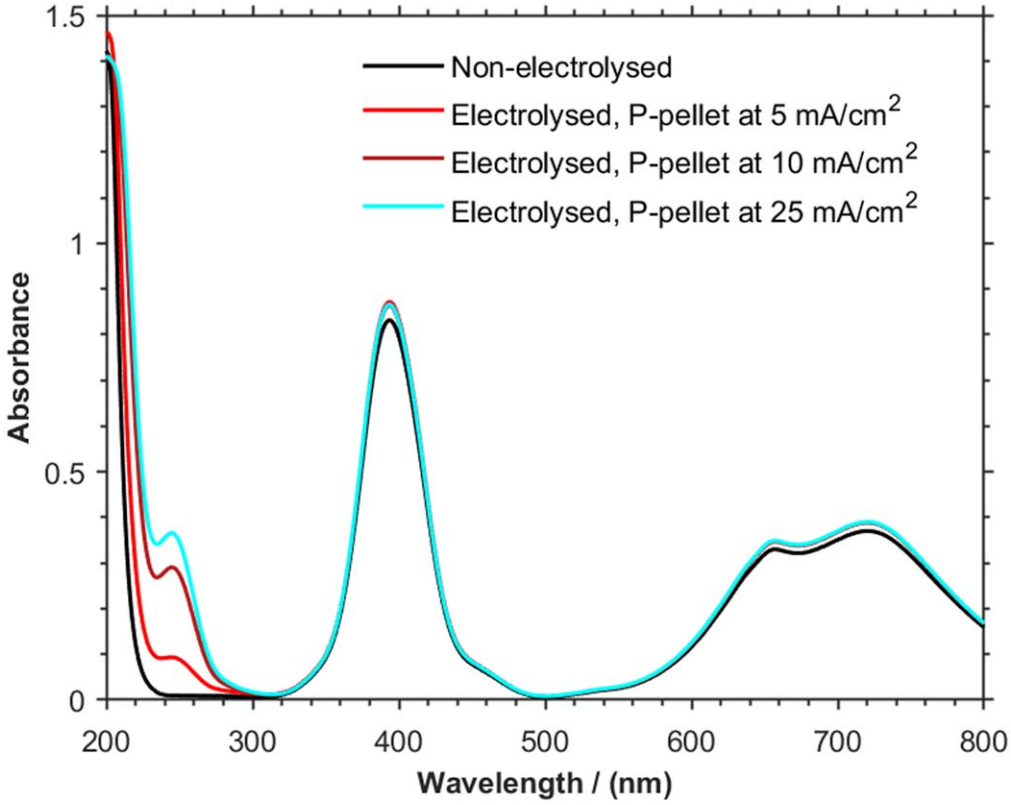

Figure 8. The UV–vis spectra for the P-Pellet before electrolysis and after an anodic charge of 500 C was passed at current densities of 5, 10 and 25 mA cm^{-2}.

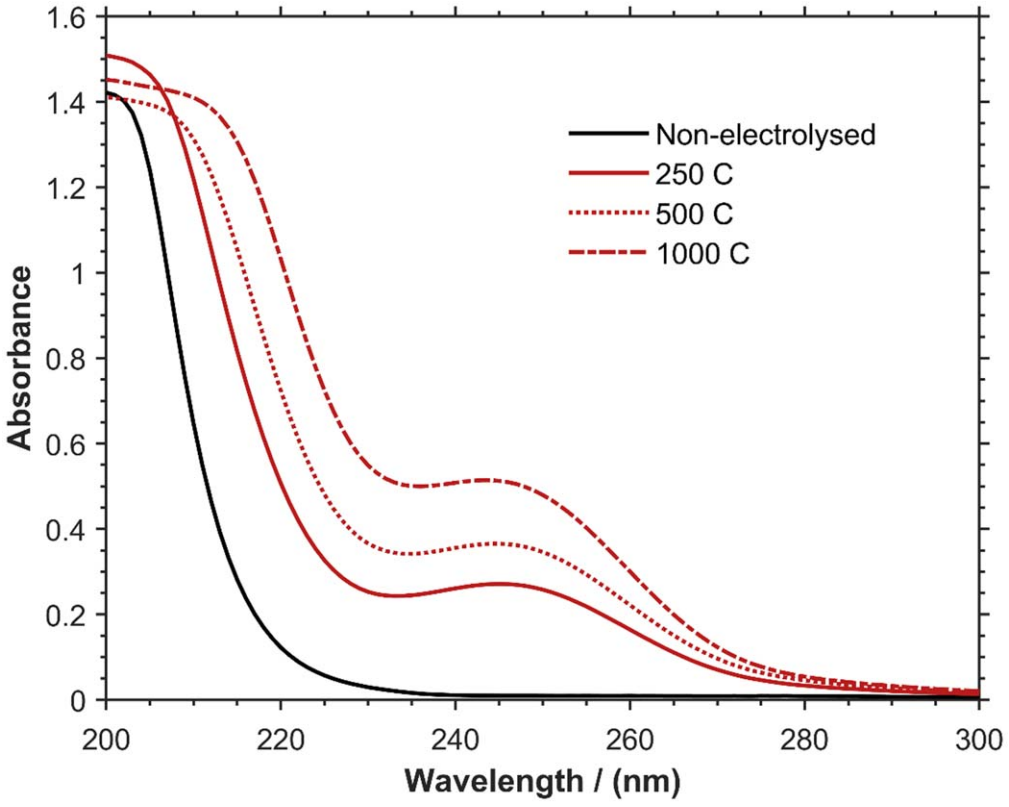

Figure 9. The UV–vis spectrum for the P-Pellet before electrolysis and after charges of 250, 500 and 1000 C were passed at a current density of 25 mA cm^{-2}.

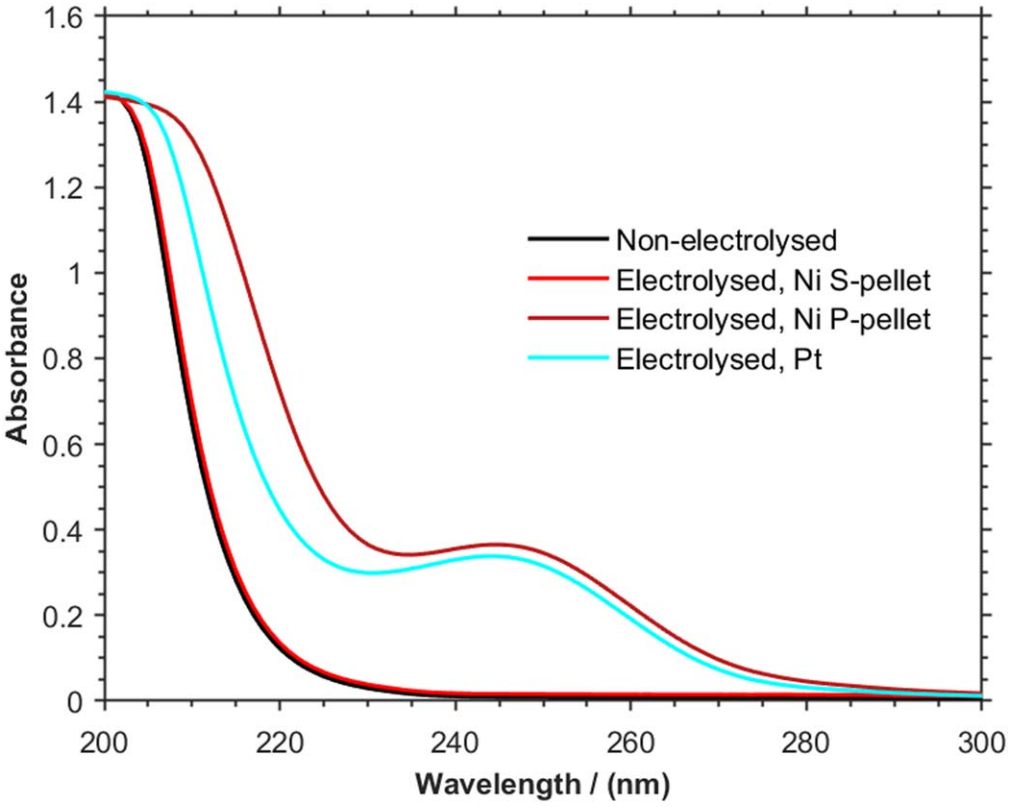

Figure 10. Comparison of the UV–vis spectrum for a platinum anode versus various Ni anode materials after a charge of 500 C was passed at a current density of 25 mA cm^{-2}.

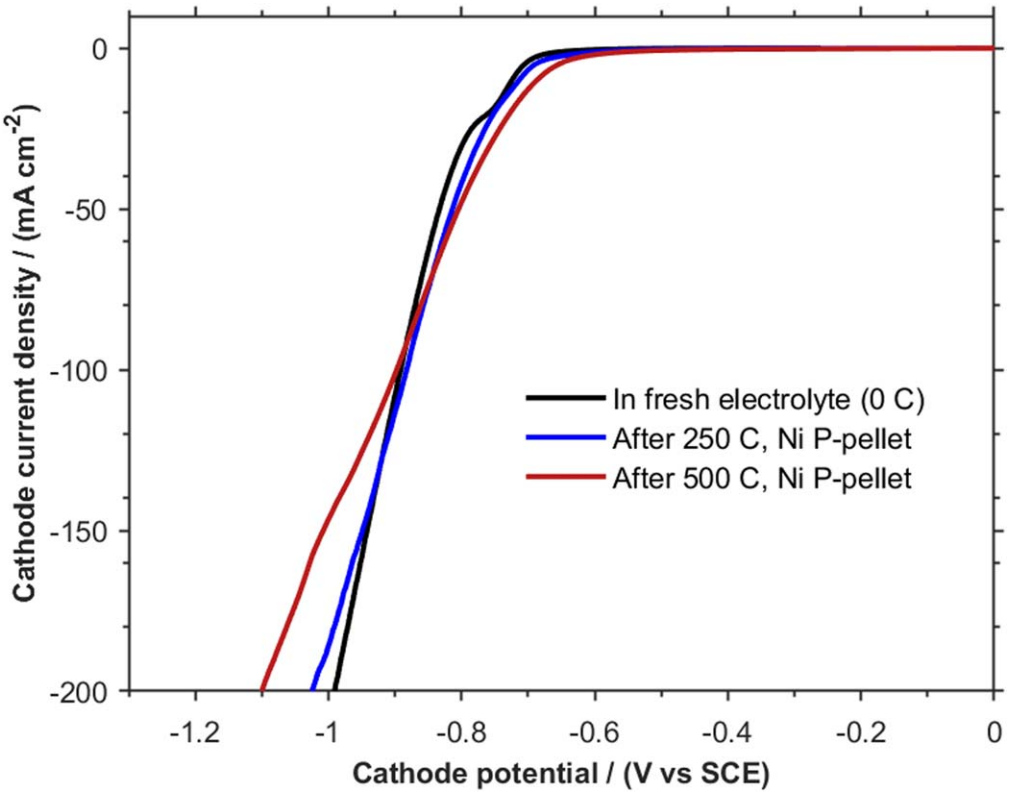

Figure 11. Polarisation plot (scan rate = 5 mV s^{-1}) for the deposition of nickel at a stainless steel cathode from the base sulfamate electrolytes, showing the influence of the amount of anodic decomposition product (represented as 0, 250, or 500 C of charge passed) on the cathodic process.

deposition studies[45] which indicate that sulfur-containing additives typically function as depolarisers (accelerators) at low over potentials, and inhibitors at higher potentials.

The nature of the sulfamate decomposition product is still uncertain and various chemical species have been proposed (Table III). In the early study of Greene[25] employing Pt and C anodes it was suggested that the oxidation of sulfamate ions initially forms hydrazine-disulfonate (HDS) as an intermediate, with azodisulfonate (ADS) as the final product. In addition, bisulfate and persulfate ($S_2O_8^{2-}$) were also formed, and the following mechanism was proposed.

$$2H_2NSO_3^- \rightarrow O_3SHN - NHSO_3^{2-} + 2H^+ + 2e - \text{ (HDS formation)} \quad [1]$$

$$2H_2NSO_3^- \rightarrow O_3SN = NSO_3^{2-} + 4H^+ + 4e - \text{ (ADS formation)} \quad [2]$$

The ADS species is not stable and can undergo hydrolysis to form nitrogen gas, bisulfite and bisulfate ions:

$$O_3SN = NSO_3^{2-} + H_2O \rightarrow N_2 + HSO_3^- + HSO_4^- \quad [3]$$

The steady-state concentration of ADS therefore depends on the relative rates of reactions [1], [2] and [3]. In the study of Greene[25] the concentration of ADS formed was typically in the range 0.5–5.0 mM, depending on the experimental conditions.

At higher anodic potentials, it is suggested that sulfamate can be oxidised to form nitrogen and sulfate ions:

$$2H_2NSO_3^- + 2H_2O \rightarrow N_2 + 2SO_4^{2-} + 8H^+ + 6e- \quad [4]$$

Finally, there is a possibility of oxidising sulfate ions directly to persulfate ions ($S_2O_8^{2-}$):

$$2SO_4^{2-} \rightarrow S_2O_8^{2-} + 2e^- \quad [5]$$

Unfortunately, standard or formal potentials are not known for any electrochemical reactions involving sulfamate ions, but for reaction [5] a value of $E^0 = 1.75$ V vs SCE is available. Approximate values for the onset potentials have, however, being measured for these reactions[46] and these reflect both thermodynamic and kinetic considerations. For reaction [1] the onset potential is 1.05 V vs SCE, 1.15 V for reaction [2] and 1.35 V for reaction [4]. These potentials were measured in a standard nickel sulfamate electroforming bath employing low-sulfur anodes and suggest that sulfamate oxidation is likely under the conditions explored in this study.

Table III. Summary of sulfamate decomposition products detected in various studies.[25,27,28,33]

Anode	Bath Composition	Products Detected	References
Pt or C	1.3 M Ni sulfamate, pH = 4	ADS, HDS, HSO_3^-, SO_4^{2-}, $S_2O_8^{2-}$	25
Pt	1.0 M Na sulfamate, pH = 2 − 12	DSS (ADS and HDS as intermediates)	28
Pt	1.0 M Na sulfamate, pH = 2–13	AUP, HDS, ADS, $S_2O_6^{2-}$	27
Pt, Ni	M Ni sulfamate, pH = 4	245 nm peak (unassigned)	33

The mechanism proposed by Greene[25] was supported by Novikov and co-workers[46] who studied sulfamate oxidation at nickel electrodes under potentiostatic conditions via anodic mass changes and analysis of the evolved gases. At low potentials ($E < 1.05$ V vs SCE) nickel dissolution dominated and the current efficiency was close to 100%. However, at higher potential ($E >$ 1.05–1.15 V) significant oxidation of sulfamate to HDS occurred lowering the current efficiency, but gases were not detected. In the potential range $1.15 < E < 1.35$ V, ADS was generated reducing the current efficiency further and a black passive film formed on the anode. Finally, at a potential of $E > 1.35$ V sulfamate was oxidised to form N_2 (detected by gas analysis) and sulfate.

A follow-up study by Jiazhu and co-workers[27] largely agreed with the mechanism proposed by Greene[25] but identified an additional product they denoted as AUP. They also detected the presence of dithionate ($S_2O_6^{2-}$) due to the oxidation of bisulfite ions:

$$2HSO_3^- \rightarrow S_2O_6^{2-} + 2H^+ + 2e^- \quad [6]$$

In a more recent investigation by Zhang[28] the decomposition product was tentatively identified as diimide S-sulfonate (DSS) by mass spectrometry, although ADS and HDS were also assumed to be present as intermediate species. These authors invoked a mechanism similar to those suggested earlier, and it was proposed that the final DSS product was formed by the reaction of dithionate ions and HDS:

$$S_2O_6^{2-} + O_3SHN - NHSO_3^{2-} + 2H^+ \rightarrow H_2N = NS_2O_3 + 2SO_4^{2-} + H_2O \quad [7]$$

The present investigation was not focussed on the exact identification of the decomposition products but Fig. 12 compares measured UV–vis absorption peaks with the reference spectrum for azodisulfonate.[25] The good agreement in peak position and shape strongly suggests that the sulfamate decomposition product is primarily ADS for both types of anodes. However, this species is only partially stable and can undergo hydrolysis via reaction [3], and this is fairly rapid at temperatures above 65 °C.[6,25] The hydrolysis reaction is also catalysed by exposure to light with a wavelength shorter than 400 nm.[47]

Additional support for this assignment is provided in Fig. 13 which shows the spectra of nickel sulfamate solutions electrolysed with a P-pellet anode after heating above 65 °C for various time periods. The decline in the 245 nm absorption peak with time is consistent with the known thermal instability of ADS and a kinetic analysis indicated that hydrolysis reaction [3] exhibits pseudo first order kinetics with a half-life of $t_{1/2} = 100$ min. There is a small residual absorbance even after several half-lives which may reflect the accumulation of the bisulfite ions that are a by-product of hydrolysis. There may also be some contribution from other minority sulfonate species (e.g. AUP or DSS) both of which are reported[27,28] to have much higher thermal stabilities than ADS.

Along with the various sulfonate compounds, the formation of persulfate ion has been inferred by Greene from UV–vis spectroscopy[25] and dithionate ions were detected by Jiazhu[27] using Raman spectroscopy. Dithionate, sulfamate and bisulfate ions do not exhibit significant absorption in the UV region[48,49] so cannot be detected using UV–vis spectroscopy. However, the persulfate and sulfite ions both display a continuous absorption features extending from 200–270 nm[25,49] and there is some evidence for these species in Figs. 9 and 10. This absorption feature is only observed when ADS is also formed (Fig. 10) and increases with the anodic charge. This behaviour is consistent with product formation via reactions [3] and [5].

Sulfate or bisulfate ions can be formed via reactions [3] and [4] and then oxidised to $S_2O_8^{2-}$, but this requires very high anodic potentials ($E^0 = 2.0$ V for reaction [6]). This corresponds to a potential of 1.75 V vs. SCE, but in all experiments performed with nickel anodes the potential did not exceed 1.5 V (Fig. 14 and Table II) and it appears unlikely that persulfate is generated via reaction [6]. In that case, the observed absorption feature most likely represents the formation of bisulfite.

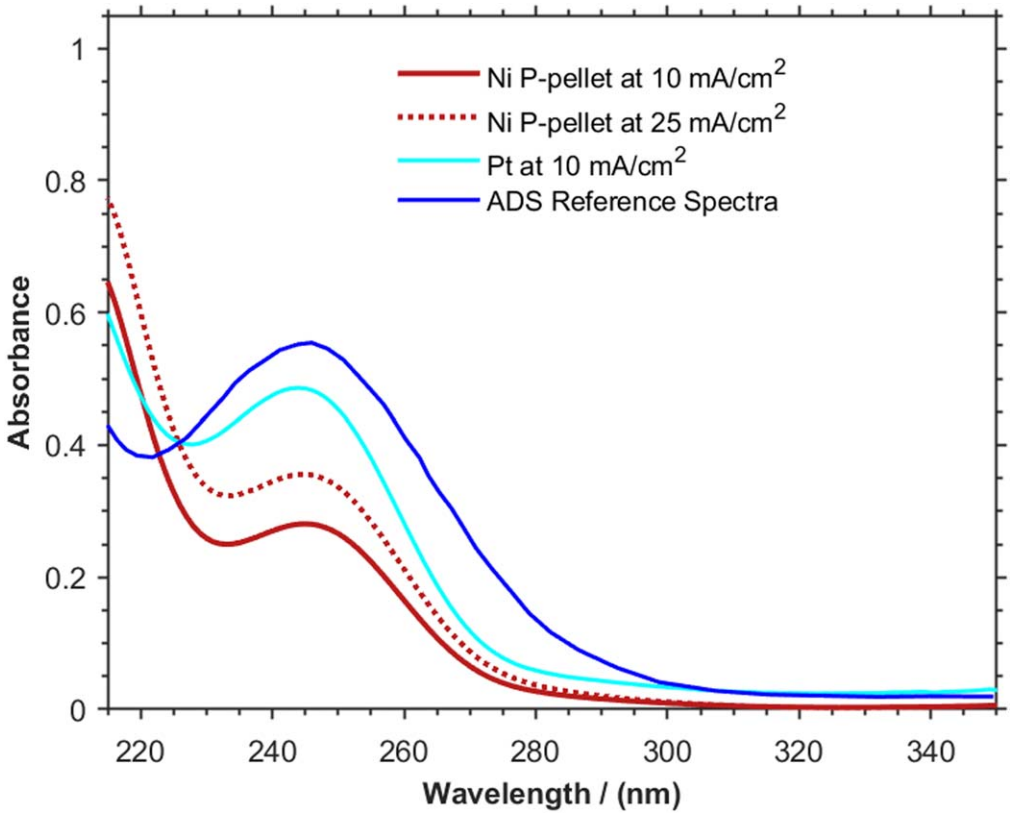

Figure 12. Comparison of the UV–Vis reference spectrum of azodisulfonate with UV absorption peaks observed in different experiments employing low-sulfur (P-Pellets) and platinum anodes. The spectra have been corrected to the non-electrolysed nickel sulfamate electrolyte.

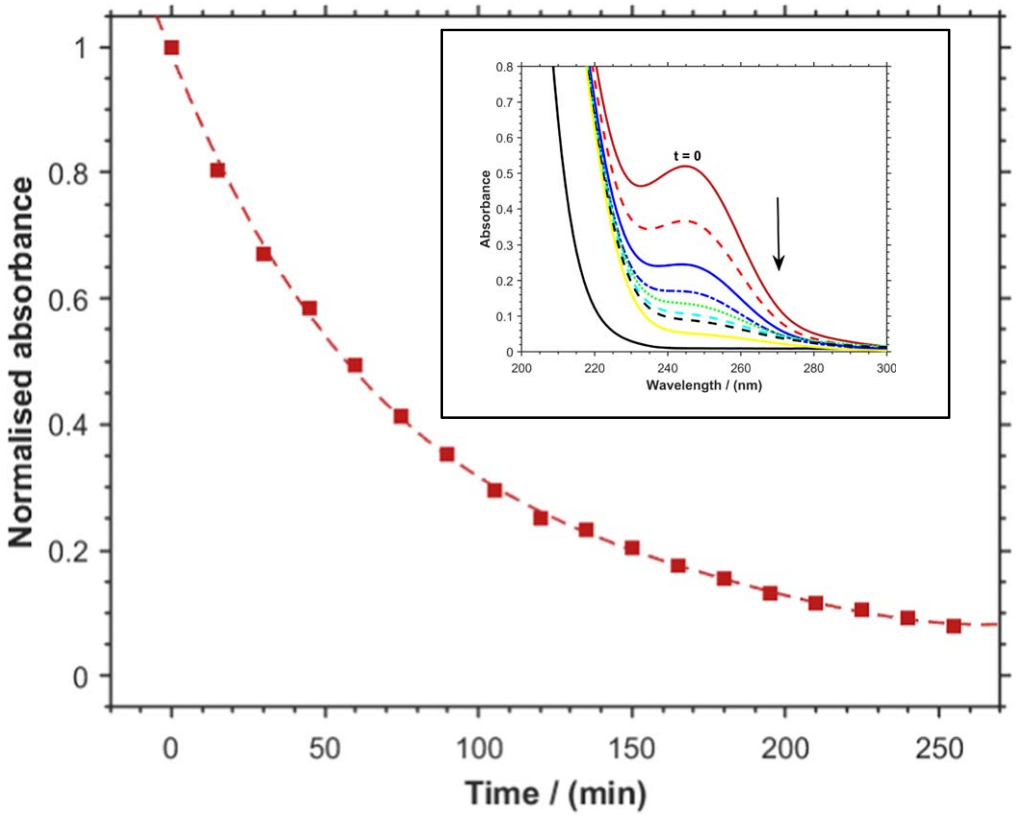

Figure 13. The decay in the normalised absorbance peak at 245 nm for a solution employing a P-pellet after heating at 67 ^{o}C for various periods. Prior to the experiment, the solutions were electrolysed at 25 mA cm^{-2} for a total charge of 500 C. The zoomed insert shows the spectral changes as a function of time.

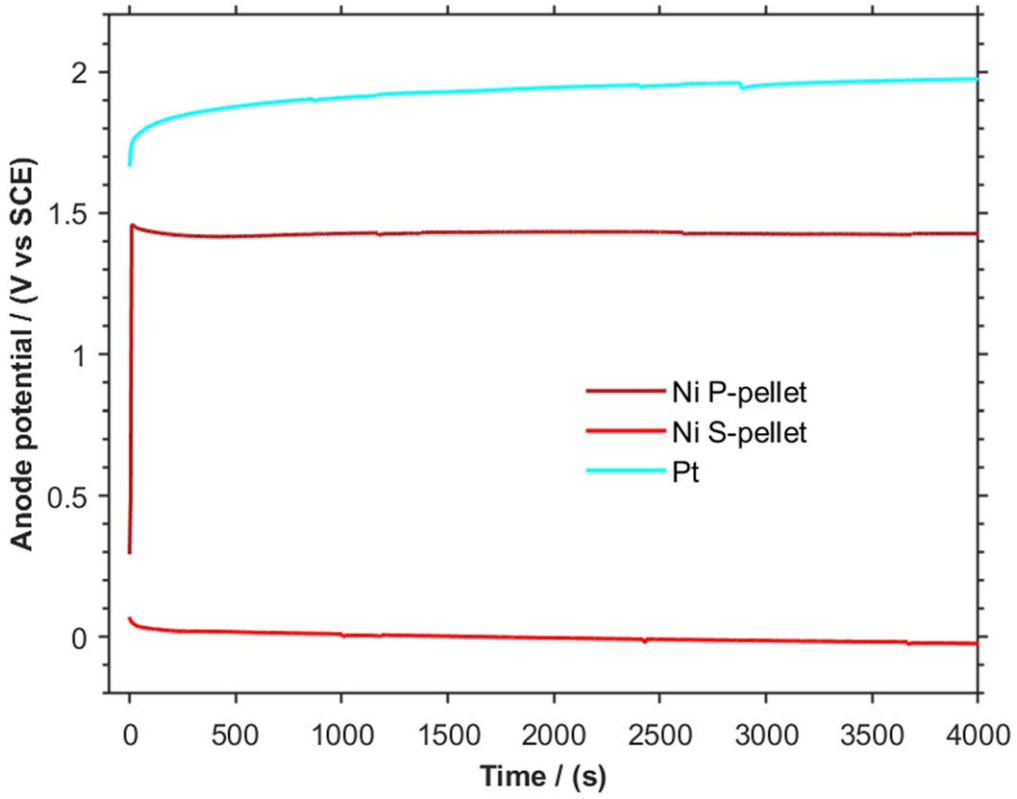

Figure 14. Anode potential as a function of time at nickel and platinum anodes for an anodic current density of 5 mA cm^{-2}. The Ni P-Pellet shows a transition from active dissolution to transpassive after 10 s.

However, for platinum anodes, where potentials in excess of 2.0 V vs SCE were often achieved (Fig. 14 and Table II) there is a possibility of direct persulfate generation alongside bisulfite formation.

Conclusions

This study has involved an investigation of various types of commercial anodes routinely employed in nickel sulfamate electroforming processes. These included examples of sulfur depolarised anodes containing approximately 0.025 wt% sulfur, and those with much lower contents (<0.0002 wt% sulfur). Initial electrochemical studies indicated that the sulfur depolarised anodes underwent dissolution in the active region and were capable of sustaining current densities in excess of 100 mA cm^{-2} without passivating, even in the absence of chloride ions or solution agitation. The anodic current efficiency was always close to 100% and the corresponding anode potential was also low. These characteristics make them ideally suited to most modern electroforming applications.

In contrast, low-sulfur content anodes showed a greater propensity to passivation and could typically only sustain low current densities (<2 mA cm^{-2}) in the active region. Moreover, the presence of chloride and solution agitation produced only a marginal improvement in dissolution characteristics. Higher current densities could only be sustained by operating under conditions where transpassive dissolution of the nickel occurred. However, due to the presence of side reactions involving sulfamate oxidation, the current efficiency was typically <100% and the anode potential was also high. These limitations make the use of low-sulfur anode materials problematic for many electroforming applications.

A second aim of the study was to investigate the sulfamate oxidation products formed under actual electroforming conditions. These products function as additives and have been shown to have an important influence on the deposit characteristics, notably with regard to stress. It was found that with sulfur depolarised anodes, such products were not detected in solution by UV–visible spectrophotometry. In these cases, the anode did not attain a sufficiently high electrode potential to oxidise the sulfamate. In contrast, the low-sulfur nickel and an inert platinum anodes attained much higher potentials and produced detectable amounts of decomposition products—as indicated by a prominent UV absorption band at 245 nm. This generation of this product was shown to be electrochemical in nature and associated with the anode reactions. The presence of the anode product was demonstrated to have an appreciable effect on the polarisation curve for nickel deposition.

The anodic decomposition products have variously been attributed to various sulfonate species, but the present results indicate that azodisulfonate is the principal species when platinum or low-sulfur nickel anodes are used. This was established on the basis of spectral characteristics and the known thermal instability of the ADS compound. Additionally, dithionate, sulfate, bisulfite and persulfate anions can also be formed at the anode. Dithionate ions could not be detected by UV–vis spectroscopy, but there was some evidence for the electrochemical formation of persulfate or sulfite. Electrochemical measurements showed that persulfate formation was not feasible at nickel anodes, but cannot be ruled out when platinum anodes are employed.

Acknowledgments

The authors would like to acknowledge Dr Tony Hart of Hart Materials for providing useful information on electroforming processes and samples of some anode materials.

ORCID

T. A. Green https://orcid.org/0000-0002-3538-5217
C. Enowmbi Tambe https://orcid.org/0000-0002-1257-6213

References

1. ASTM Standard, B374-21, *Standard Terminology Relating to Electroplating*, ASTM International.
2. R. Parkinson, "NiDI Technical Series N° 10 084." *Nickel Development Institute*, (1998).
3. D. P. Davies and S. L. Jenkins, *Mater. Sci. Eng. A*, **607**, 341 (2014).
4. G. Valsecchi, "Electroforming in Space and Ground Telescopes." *ECSarXiv*, **2020**, 1 (2020), ECS PrePrint.
5. T. Hart, *Jahrbuch Oberflachemtechnik, Band 74*, ed. T. Sorgel and E. G. Leuze Verlag (2018).
6. S. Watson, *Trans. IMF*, **67**, 89 (1989).
7. S. Roy and E. Andreou, *Curr. Opin. Electrochem.*, **20**, 108 (2020).
8. M. J. Sole, *JOM*, **46**, 29 (1994).
9. J. A. McGeough, M. C. Leu, K. P. Rajurkar, A. K. M. De Silva, and Q. Liu, *CIRP Ann.*, **50**, 499 (2001).
10. S. Watson, *Trans. IMF*, **77**, 10 (1999).
11. A. Maner and W. Ehrfeld, *Mater. Manuf. Process*, **4**, 527 (1989).
12. L. T. Romanikiw, *Plat. Surf. Fin.*, **84**, 10 (1997).
13. H. Zhang, N. Zhang, M. Gilchrist, and F. Fang, *J. Micromech. Microeng.*, **30**, 103002 (2020).
14. E. Shalyt, J. Wang, V. Parekh, and M. MacEwan, *ECS Meet. Abstr:*, **MA201402** (1714).
15. G. A. Di, *Bari, in Modern Electroplating*, ed. M. Schlesinger and M. Paunovich (Wiley, Hoboken) 5th ed. (2010).
16. R. A. F. Hammond, *Electrodeposition from Nickel Sulfamate Solutions, Technical Report* (INCO Ltd.) (1971).
17. N. V. Mandich and D. W. Braudrand, *Plat. Surf. Fin.*, **89**, 68 (2002).
18. D. Braudrand, *Met. Fin.*, **94**, 15 (1996).
19. W. Yang, Y. Luo, C. Wang, B. Wang, and W. Tian, *Mater. Des.*, **93**, 91 (2016).
20. J. K. Luo, M. Pritschow, A. J. Flewitt, S. M. Spearing, N. A. Fleck, and W. I. Milne, *J. Electrochem. Soc.*, **153**, D155 (2006).
21. J. J. Kelly, S. H. Goods, A. A. Talin, and J. T. Hachman, *J. Electrochem. Soc.*, **153**, C318 (2006).
22. S. H. Goods, J. J. Kelly, A. A. Talin, J. R. Michael, and R. M. Watson, *J. Electrochem. Soc.*, **153**, C325 (2006).
23. Z. Rao, S. J. Hearne, and E. Chason, *J. Electrochem. Soc.*, **166**, D3212 (2019).
24. J. L. Marti, *Plating*, **53**, 61 (1966).
25. A. F. Greene, *Plating*, **55**, 594 (1968).
26. O. J. Klingenmaier, *Plating*, **52**, 1138 (1965).
27. L. Jiazhu, Z. Haiyan, and Z. Liangyu, *Plat. Surf. Fin.*, **77**, 54 (1990).
28. H. Zhang and S.-M. Park, *J. Appl. Electrochem.*, **24**, 1182 (1994).
29. M. Datta and I. B. M. J. Res., *Develop.*, **37**, 207 (1993).
30. A. C. Hart, *Trans. IMF*, **51**, 69 (1973).
31. A. C. Hart, *Personal Communication* (2020).
32. A. C. Hart, W. R. Wearmouth, and A. C. Warner, *Trans. IMF*, **54**, 56 (1976).
33. H. Nakano, S. Oue, S. Kobayashi, T. Akiyama, H. Fukushima, A. Kubota, and T. Inoue, *J. Surface Finish. Soc. Jpn.*, **54**, 533 (2003).
34. G. A. Di Bari and J. V. Petrocelli, *J. Electrochem. Soc.*, **112**, 99 (1965).
35. M. G. Moula, G. Szymanski, B. Shobeir, H. Huang, I. J. Burgess, A. Chen, and J. Lipkowski, *Electrochim. Acta*, **162**, 108 (2015).
36. A. Morrison, J. J. Leitch, G. Szymanski, G. Moula, B. Barlow, I. J. Burgess, B. Shobeir, H. Huang, and J. Lipkowski, *Electrochim. Acta*, **260**, 684 (2018).
37. C. M. Whittington, K. L. L. Yeung, and W. Y. Lo, *Trans. IMF*, **89**, 122 (2011).
38. G. A. DiBari, *Plat. Surf. Fin.*, **86**, 32 (1999).
39. P. Russell and J. Newman, *J. Electrochem. Soc.*, **134**, 1051 (1987).
40. H. Kaesche, *Corrosion of Metals* (Springer, Berlin) p.237 (2003).
41. N. Sato and G. Okamoto, *J. Electrochem. Soc.*, **110**, 605 (1963).
42. A. K. N. Reddy and B. Rao, *Can. J. Chem.*, **47**, 2687 (1969).
43. J. Wang, D. R. Gabe, A. C. Hart, and P. C. Crouch, *Trans. IMF*, **91**, 4 (2013).
44. I. Burgess, B. Barlow, G. Szymanski, J. Lipkowski, B. Shobeir, and B. Love, *J. Electrochem. Soc.*, **163**, C164 (2016).
45. S.-K. Kim, J. E. Bonevish, D. Josell, and T. P. Moffat, *J. Electrochem. Soc.*, **154**, D443 (2007).
46. L. Novikov, G. Kurnoskin, V. Flerov, G. Shulypin, and I. Ivashkina, *Zashch. Met.*, **25**, 871 (1989).
47. H. Higashino and H. Ohkawa, *US Patent 4*, **696**, 721 (1987).
48. S. J. Waygood and W. J. McElroy, *J. Chem. Soc. Faraday Trans.*, **88**, 1525 (1992).
49. R. P. Buck, S. Singhadeja, and L. B. Rogers, *Anal. Chem.*, **26**, 1240 (1954).